
Since January 2020 Elsevier has created a COVID-19 resource centre with free information in English and Mandarin on the novel coronavirus COVID-19. The COVID-19 resource centre is hosted on Elsevier Connect, the company's public news and information website.

Chemical Physics Letters 507 (2011) 134–137

Contents lists available at ScienceDirect

Chemical Physics Letters

journal homepage: www.elsevier.com/locate/cplett

# Increased dispersion and solubility of carbon nanotubes noncovalently modified by the polysaccharide biopolymer, chitosan: MD simulations

Thanyada Rungrotmongkol [a,g], Uthumporn Arsawang [a], Chularat Iamsamai [b], Arthit Vongachariya [c], Stephan T. Dubas [d,g], Uracha Ruktanonchai [e], Apinan Soottitantawat [f], Supot Hannongbua [a,g,*]

[a] Computational Chemistry Unit Cell, Department of Chemistry, Faculty of Science, Chulalongkorn University, Bangkok 10330, Thailand
[b] Doctor of Philosophy Program in Nanoscience and Technology, Graduate School, Chulalongkorn University, Bangkok 10330, Thailand
[c] UBE Technical Center (Asia) Limited, UBE Group (Thailand), Rayong 21000, Thailand
[d] Metallurgy and Materials Science Research Institute, Chulalongkorn University, Bangkok 10330, Thailand
[e] National Nanotechnology Center, National Science and Technology Development Agency, Pathumthani 12120, Thailand
[f] Department of Chemical Engineering, Faculty of Engineering, Chulalongkorn University, Bangkok 10330, Thailand
[g] Center of Innovative Nanotechnology, Chulalongkorn University, Bangkok 10330, Thailand

ARTICLE INFO

*Article history:*
Received 16 November 2010
In final form 21 March 2011

ABSTRACT

In order to explain the solubility of carbon nanotubes (CNT), including single walled CNTs, wrapped with chitosan of a 60% degree of deacetylation, MD simulations were applied to represent three chitosan concentrations, using two pristine CNTs (*p*CNT–*p*CNT), and one and two CNTs wrapped (*p*CNT–*cw*CNT and *cw*CNT–*cw*CNT). The CNT aggregation was observed in *p*CNT–*p*CNT and *p*CNT–*cw*CNT due to van der Waals interactions between tube–tube aromatic rings, and inter-CNT bridging by chitosan, respectively. At higher chitosan concentrations, such that most to all of CNTs were wrapped with chitosan, charge–charge repulsion was found to separate robustly the *cw*CNTs and lead to a well dispersed solution.


## 1. Introduction

Since the discovery of carbon nanotubes (CNTs) by Iijima in 1991 [1], they have been widely studied, with the different properties of single walled (SWCNT), double walled and multiple walled CNTs being characterized, and gained a great number of applications, such as in electronic circuits (especially SWCNTs), nanocomposites, sensor devices, smart textiles and drug delivery systems. However, CNTs are poorly solvated in any solvent but rather they tend to aggregate due to the van der Waals' interactions between the CNTs. Therefore, surface modification of CNTs is required to overcome this vital problem. Both covalent and noncovalent surface modifications have been shown to be effective approaches and provide a wide variety of functional groups on the surface of CNTs, improving the dispersion efficiency and the stability of modified CNTs in aqueous solution [2,3]. Whilst covalent modifications may be unsuitable for SWCNT due to the creation of 'holes' in the wall, noncovalent surface modification has been found to be an effective way to preserve the integrity of SWCNTs and in particular their electronic properties [4]. However, to accelerate the optimal development and application of CNTs, it is required to understand at the molecular level how polysaccharide biopolymers, such as chitosan, can provide a high dispersion efficiency and stability of CNTs in aqueous solution through wrapping on the outer surface of the CNTs including SWCNTs [5].

Surfactants, as sodium dodecylsulfate or sodium benzoylsulfonate [6,7], polyelectrolytes, such as polystyrene sulfonate, polydiallyldimethyl ammonium chloride and polyethyleneimine [8–10], and even biopolymers, as chitosan [11,12], gelatin [13] and gum arabic [14], have been successfully used as dispersing agents to increase the solubility of CNTs through noncovalent interactions. The wrapping phenomenon of modified CNTs (including SWCNTs) with various polymers has frequently been proposed in both theoretical and experimental works [15,16]. Such wrapping polymers include synthetic polymers, such as poly(*m*-phenylenevinylene-*co*-2,5-dioctyloxy-*p*-phenylenevinylene) (PmPV) [15] and poly(*p*-phenylenevinylene) (PPV) [17], as well as natural polymers, such as the polysaccharides amylase [18], alginate [19] and chitosan [20].

Since chitosan presents a good biocompatibility, is readily available and is a relatively cheap and renewable resource, it has been widely used to improve SWCNT dispersion in electrochemical electrodes, the manufacture of biosensors and drug delivery applications [21–23]. Recently, Iamsamai et al. reported that chitosan with a 61% degree of deacetylation (DD) is more favorably adsorbed onto the surface of CNTs than that of 93% DD chitosan,

* Corresponding author at: Computational Chemistry Unit Cell, Department of Chemistry, Faculty of Science, Chulalongkorn University, Bangkok 10330, Thailand. Fax: +66 22 187603.
*E-mail address:* supot.h@chula.ac.th (S. Hannongbua).

0009-2614/$ - see front matter © 2011 Elsevier B.V. All rights reserved.
doi:10.1016/j.cplett.2011.03.066

possibly because of their cumulative hydrophobic parts [24]. In addition, CNTs wrapped with 61% DD chitosan (*cw*CNT) were found to be highly dispersed and remain stable at aqueous concentrations of more than 1 mM. However, no explanation at the molecular level for that behavior in aqueous solutions is currently available.

Molecular dynamics (MD) simulation is a specific tool for providing detailed theoretical information at the molecular level, and is especially relevant and useful for biological systems which are hard to access experimentally. As a testament to the suitability of MD approaches to biological systems, success has already been attained with evaluation of the interaction (loading and release) of anticancer drugs carried by CNT [25], as well as the ligand–enzyme interactions in viral influenza [26], human immunodeficiency virus type 1 (HIV-1) [27], severe acute respiratory syndrome coronavirus (SARS-coV) [28] and chikungunya virus (CHIKV) [29].

In the present report, MD simulation was applied to acquire detailed molecular information so as to try to understand and explain the solubility of the SWCNT wrapped with 60% DD chitosan (*cw*CNT) as a function of the bound chitosan: SWCNT ratio and concentration. There are three different theoretical chitosan concentrations, using two pristine SWCNTs (*p*CNT–*p*CNT), and one and two CNTs wrapped (*p*CNT–*cw*CNT) and (*cw*CNT–*cw*CNT) as representative model components from a very low to no chitosan concentration, a chitosan to SWCNT ratio and concentration such that ~50% of SWCNT molecules exist as *cw*CNT, and an excess of chitosan such that all SWCNT molecules are *cw*CNT, respectively. The results were extensively analyzed and discussed in terms of the displacement between two SWCNTs, tube–tube orientation and the solvation properties of chitosan fragments relative to those of pristine SWCNTs (*p*CNT–*p*CNT).

## 2. Materials and methods

The 60% DD chitosan and the (8,8) armchair SWCNTs with a diameter of 11 Å, chiral vectors $n = 8$ and $m = 8$, and 12 repeating units were constructed using the Material Studio 4.3 package. The 60%DD chitosan containing 12 D-glucosamine (GLS or G) and 8 *N*-acetyl-D-glucosamine (NAG or N) with the random symmetric sequence of GGNGNGNGGNGNGNGNGG was used in this study. The three models, as shown in Figure 1, are (a) two pristine SWCNTs (*p*CNT–*p*CNT), (b) a pristine SWCNT – chitosan wrapped SWCNT (*p*CNT–*cw*CNT), and (c) two chitosan wrapped SWCNTs (*cw*CNT–*cw*CNT). Each model was solvated in an aqueous solution. To neutralize the *p*CNT–*cw*CNT and *cw*CNT–*cw*CNT systems, the chloride ions were added using the LEaP module of AMBER. The MD simulations were set up and carried out as previously reported [25]. The SWCNTs and chitosan were parameterized by AMBER03 [30] and GLYCAM06 [31] force fields, respectively. The SPC/E water model, with an octagonal box over 12 Å from the surface of the CNTs or chitosan–CNT complexes, was applied. Then the solvated box edges were set to 68.0, 80.4 and 91.6 Å in the *p*CNT–*p*CNT, *p*CNT–*cw*CNT and *cw*CNT–*cw*CNT systems, respectively. The simulations were calculated using the AMBER10 program package [32] with the *NPT* ensemble (constant number of atoms, pressure and temperature) at 1 atm and a time step of 2 fs. The SHAKE algorithm was applied to all bonds involving hydrogen atoms to constraint their motions. Periodic boundary conditions were applied and the cutoff function was set at 12 Å for nonbonded interactions with the particle mesh Ewald method. The whole system was heated from 10 to 300 K for 200 ps and equilibrated at 300 K for 5 ns. Finally, the production stage was performed until 20 ns and the structural coordinates were saved every 1 ps for analysis.

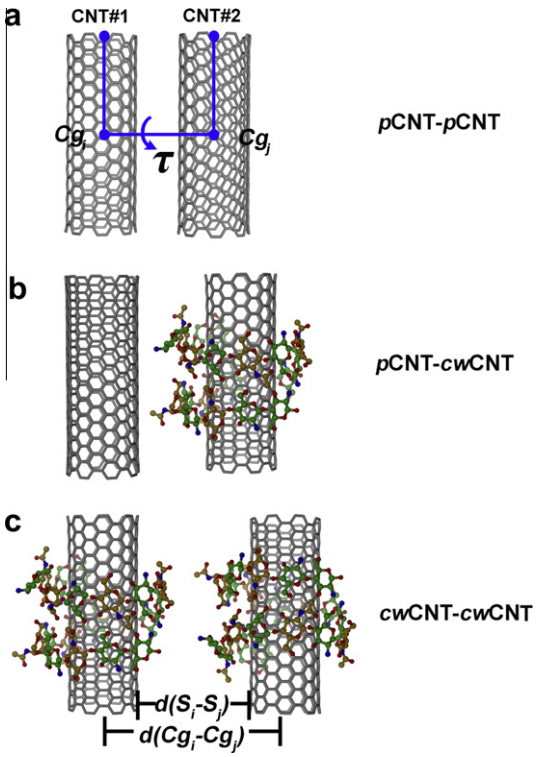


**Figure 1.** Schematic views of (a) two pristine SWCNTs (*p*CNT–*p*CNT), (b) *p*CNT–*cw*CNT and (c) *cw*CNT–*cw*CNT, where the SWCNT (labeled CNT in the figure) and the polymer used are the (8,8) armchair and 60% DD chitosan, respectively. The distances ($d(Cg_i\text{–}Cg_j)$) and ($d(S_i\text{–}S_j)$) and the torsion angle ($\tau$) between the two SWCNTs were defined through the center of gravity (*Cg*) and the surface of each tube in which $\tau = 0°$ means the two tubes are parallel.

## 3. Results and discussion

### 3.1. Dispersion and solubility of SWCNTs

In order to understand the chitosan-assisted dispersion and separation of the SWCNTs in aqueous solution, the tube–tube displacement and orientation were monitored in terms of the distance from the center of gravity of the *i*th tube ($Cg_i$) to that of the *j*th tube ($Cg_j$), $d(Cg_i\text{–}Cg_j)$, and the torsion angle between the two SWCNTs' axis, $\tau$, respectively, as defined in Figure 1. The calculated results are summarized in Figure 2.

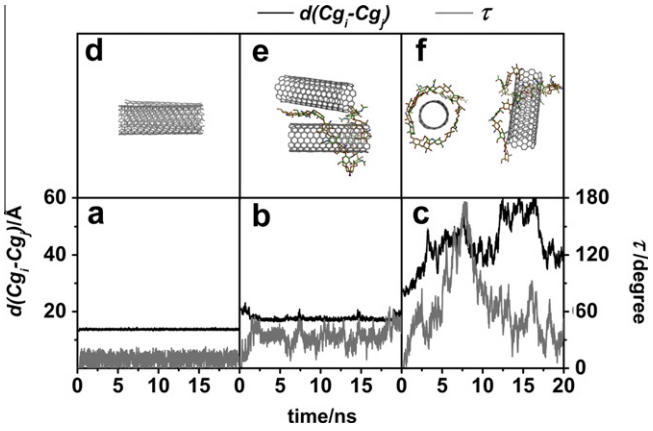


**Figure 2.** Distance, $d(Cg_i\text{–}Cg_j)$, between the two centers of gravity of SWCNT and torsion angle, $\tau$ (see Figure 1 for definition), as a function of the simulation time for the three systems, (a) *p*CNT–*p*CNT, (b) *p*CNT–*cw*CNT and (c) *cw*CNT–*cw*CNT, where their corresponding structures taken from the MD simulations are also shown (d–f).

With the no chitosan (or very low chitosan: CNT bound ratio) model system of *p*CNT–*p*CNT, the averaged tube–tube displacement represented by the distance between the tube centers of gravity, $d(Cg_i–Cg_j)$, was ~14 Å, which is equivalent to a distance between the tube surfaces, $d(S_i–S_j)$, of 3 Å (Figure 2a). In addition, the tilt angle designated by the torsion $\tau$ angle is ~11°. These values are almost constant over the entire simulation period. The $\tau$ data indicated that the two pristine SWCNTs were oriented in an almost parallel configuration (Figure 2d), whilst the distance between the surfaces of the two SWCNTs ($d(S_i–S_j)$ = ~3 Å) implied that the hydrophobic and van der Waals interactions between the aromatic rings of both CNTs played a role. This provides a clear answer as to why the *p*CNTs (and so by likely extrapolation, *p*CNTs in general) were found to aggregate experimentally in solution.

With an inadequate concentration of chitosan, such that a bound ratio of chitosan: CNT of ~1:2 was attained, represented by the model *p*CNT–*cw*CNT system in this MD simulation approach, the $d(Cg_i–Cg_j)$ was increased by ~3 Å (from 14 to 17 Å) and the tilt angle was increased from 11 to 33°, relative to the *p*CNT–*p*CNT system. Interestingly, one end of the chitosan was found to unwrap from the modified tube (CNT#2 in Figure 1b) and change its configuration to interact with the *p*CNT (CNT#1 in Figure 1b), *i.e.*, the chitosan rearranges its conformation to locate in between and interact with both SWCNTs (Figure 2e). Although the $d(Cg_i–Cg_j)$ distance of ~17 Å, with the corresponding $d(S_i–S_j)$ of ~6 Å, is rather long for molecular interactions between the two SWCNTs, the detected CNT#1–chitosan–CNT#2 configuration signifies that chitosan can act as the linker bridging the tubes together.

The situation is dramatically different for the model system where both SWCNTs were wrapped by chitosan (*cw*CNT–*cw*CNT), used to represent SWCNTs in a solution with a sufficiently high enough concentration of chitosan that almost all SWCNT molecules are wrapped (*cw*CNT). In this system the MD simulation revealed that the two *cw*CNTs were totally separate and freely rotating (Figure 2f), *i.e.*, the noncovalent modified *cw*CNTs are highly soluble, supported by the $d(Cg_i–Cg_j)$ distance (~35–60 Å) and the $\tau$ angle (~60–180°), as seen in Figure 2c. The high dispersion and solubility levels of the two *cw*CNTs are mainly due to the strong repulsive interactions between the positively charged ammonium groups of the glucosamine units on each *cw*CNT.

### 3.2. Role of chitosan fragments

According to a previous study on chitosan-modified CNTs [24], the binding mechanism of chitosan wrapping on the outer surface of CNTs is thought to be due to the hydrophobic interactions between the acetyl groups of chitosan and the aromatic rings of the CNT. In order to provide detailed information at the molecular level so as to understand the mechanism of action, the atom–atom radial distribution function (RDF, $g_{xy}(r)$), that is the probability of finding a particle of type *y* within a sphere radius *r* around the particle of type *x*, were calculated. Here, *x* represents the nitrogen atoms of chitosan fragments (the *N*-acetyl-D-glucosamine (NAG), and D-glucosamine (GLS)), and *y* denotes all the carbon atoms of the wrapped SWCNTs (only the *cw*CNTs shown in Figure 1, CNT#2 for the *p*CNT–*cw*CNT and both CNT#1 and CNT#2 for the *cw*CNT–*cw*CNT) or the water oxygen atoms. The results are plotted and compared in Figure 3.

In the *p*CNT–*cw*CNT system (Figure 3a), the RDF plots from the *N* atom on the acetyl group of the NAG unit, N(NAG), and the ammonium group of the GLS unit, N(GLS), to all carbon atoms of the wrapped SWCNT show broad maxima at 5.2 Å (black line) and 5.7 Å (gray line) with high and low intensities, respectively. This means that the hydrophobic acetyl group of NAG can approach closer to and interact with the outer surface of the SWCNTs

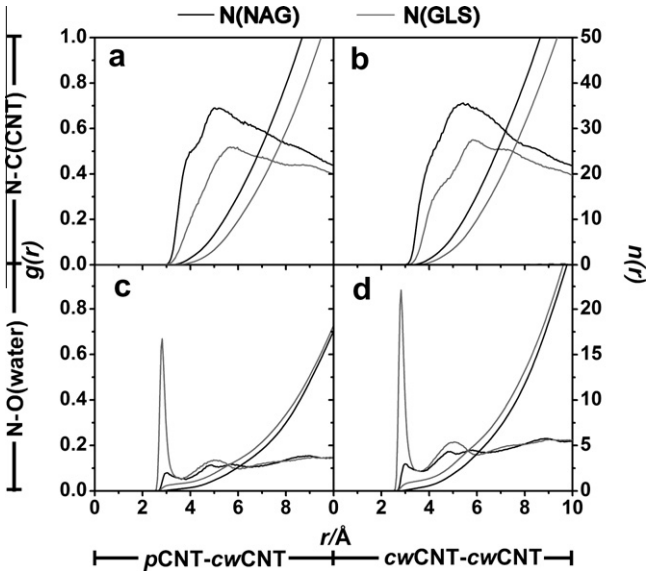


**Figure 3.** RDFs from the nitrogen atoms on the *N*-acetyl-D-glucosamine (N(NAG), black line) and D-glucosamine (N(GLS), gray line) of chitosan to the carbon atoms of the *cw*CNTs (a) CNT#2 for *p*CNT–*cw*CNT, (b) both CNT#1 and CNT#2 for *cw*CNT–*cw*CNT and the oxygen atoms of water for (c) *p*CNT–*cw*CNT and (d) *cw*CNT–*cw*CNT.

through van der Waals interactions than the hydrophilic ammonium group (GLS). Similarly for the *cw*CNT–*cw*CNT system (Figure 3b), the maximum RDF for the NAG (5.6 Å, black line) takes place at a shorter distance than that of the GLS (6.2 Å, gray line) with a higher density and coordination number. It is interesting that these N(NAG)–C(CNT) and N(GLS)–C(CNT) distances of the *cw*CNT–*cw*CNT system are longer than those of the *p*CNT–*cw*CNT system, respectively. This fact can be explained using the molecular configurations shown in Figure 2e and f, as that the chitosan in the highly soluble *cw*CNT–*cw*CNT system can be accessed by water molecules much more easily than in the aggregated *p*CNT–*cw*CNT system. This solvation effect then pulls the chitosan fragments in the *cw*CNT–*cw*CNT system out to a longer distance from the SWCNT outer surface than that of the *p*CNT–*cw*CNT one.

As expected for the both systems containing chitosan, the RDFs for the N(GLS) are much sharper with much higher density than those of the N(NAG) (gray and black lines, respectively, in Figure 3c and d). The corresponding running integration number, the number of water molecules at the distance *r*, around the neutral NAG is lower than that of the positively charged GLS at all distances. The corresponding coordination numbers, integrated to the first minima, of the N(NAG) and N(GLS) for both systems are 0.3 and 0.9 water molecules.

## 4. Conclusions

A MD simulation approach was applied to investigate the increase in dispersion and solubility of SWCNT when wrapped with 60% DD chitosan as the chitosan concentration is increased. The calculated distance between the centers of each SWCNT and the tube–tube orientation for the three modeled systems, *p*CNT–*p*CNT, *p*CNT–*cw*CNT and *cw*CNT–*cw*CNT, indicate the *p*CNT aggregates due to the hydrophobic and van der Waals interactions between the aromatic rings of the *p*CNTs. For the *p*CNT–*cw*CNT, the chitosan on the *cw*CNT#2 was found to act as a linker to bridge the *p*CNT#1 and *cw*CNT#2 together to aggregate. In contrast, in the high-concentration chitosan model (*cw*CNT–*cw*CNT) the two *cw*CNTs were totally separated, freely rotated and well dispersed in the aqueous solution owing to the charge–charge repulsive force of the ammo-

nium groups of GLS, with a fragment of the 60% DD chitosan wrapped on each tube. Interestingly, the hydrophobic acetyl group of the NAG fragment is likely to interact with the aromatic rings of the carbon nanotube via van der Waals interactions while the positively charged ammonium group of GLS fragment was strongly hydrated by water molecules.

## Acknowledgments

This work was supported by the National Research University Project of CHE and Ratchadaphiseksomphot Endowment Fund (HR1155A) and the Thai Government Stimulus Package 2 (TKK2555), under the Project for Establishment of Comprehensive Center for Innovative Food, Health Products and Agriculture. T.R. thanks the postdoctoral fellowship from the Ratchadaphiseksomphot Endowment Fund from Chulalongkorn University, and the TRF Grant for New Research (Grant No. TRG5280035). C.I. thanks Thailand Graduate Institute of Science and Technology (TGIST Grant No. TG-55-09-50-059D), and The 90th Anniversary of Chulalongkorn University Fund (Ratchadaphiseksomphot Endowment Fund). The Center of Excellence for Petroleum, Petrochemicals and Advanced Materials, Chulalongkorn University is acknowledged.

## References

[1] S. Iijima, Nature (London) 354 (1991) 56.
[2] J.L. Bahr, J.M. Tour, J. Mater. Chem. 12 (2002) 1952.
[3] M.O. Lisunova, N.I. Lebovka, O.V. Melezhyk, Y.P. Boiko, J. Colloid Interface Sci. 299 (2006) 740.
[4] Y.-L. Zhao, J.F. Stoddart, Acc. Chem. Res. 42 (2009) 1161.
[5] Q. Yang, L. Shuai, X. Pan, Biomacromolecules 9 (2008) 3422.
[6] V.C. Moore, M.S. Strano, E.H. Haroz, R.H. Hauge, R.E. Smalley, J. Schmidt, Y. Talmon, Nano Lett. 3 (2003) 1379.
[7] J. Yu, N. Grossiord, C.E. Koning, J. Loos, Carbon 45 (2007) 618.
[8] X. Hu, T. Wang, X. Qu, S. Dong, J. Phys. Chem. B 110 (2006) 853.
[9] D.-Q. Yang, J.-F. Rochette, E. Sacher, J. Phys. Chem. B 109 (2005) 4481.
[10] S. Zhan, Y. Li, J. Dispers. Sci. Technol. 29 (2008) 240.
[11] T. Takahashi, C.R. Luculescu, K. Uchida, T. Ishii, H. Yajima, Chem. Lett. 34 (2005) 1516.
[12] H. Yang, S.C. Wang, P. Mercier, D.L. Akins, Chem. Commun. (2006) 1425.
[13] W. Zheng, Y.F. Zheng, Electrochem. Commun. 9 (2007) 1619.
[14] R. Bandyopadhyaya, E. Nativ-Roth, O. Regev, R. Yerushalmi-Rozen, Nano Lett. 2 (2002) 25.
[15] M. Yang, V. Koutsos, M. Zaiser, J. Phys. Chem. B 109 (2005) 10009.
[16] S.S. Tallury, M.A. Pasquinelli, J. Phys. Chem. B 114 (2010) 4122.
[17] W. Liu, C.-L. Yang, Y.-T. Zhu, M.-S. Wang, J. Phys. Chem. C 112 (2008) 1803.
[18] Y.H. Xie, A.K. Soh, Mater. Lett. 59 (2005) 971.
[19] Y. Liu, C. Chipot, X. Shao, W. Cai, J. Phys. Chem. B 114 (2010) 5783.
[20] F. Peng, F. Pan, H. Sun, L. Lu, Z. Jiang, J. Memb. Sci. 300 (2007) 13.
[21] J. Chen, G. Yang, M. Chen, W. Li, Russ. J. Electrochem. 45 (2009) 1287.
[22] X. Zhang, L. Meng, Q. Lu, Z. Fei, P.J. Dyson, Biomaterials 30 (2009) 6041.
[23] G. Zhao, X. Zhan, Electrochim. Acta 55 (2010) 2466.
[24] C. Iamsamai, S. Hannongbua, U. Ruktanonchai, A. Soottitantawat, S.T. Dubas, Carbon 48 (2010) 25.
[25] U. Arsawang, O. Saengsawang, T. Rungrotmongkol, P. Sornmee, T. Remsungnen, S. Hannongbua, J. Mol. Graph. Model. 29 (2011) 591.
[26] T. Rungrotmongkol et al., Biochem. Biophys. Res. Commun. 385 (2009) 390.
[27] T. Rungrotmongkol, A.J. Mulholland, S. Hannongbua, J. Mol. Graph. Model. 26 (2007) 1.
[28] V. Nukoolkarn, V.S. Lee, M. Malaisree, O. Aruksakulwong, S. Hannongbua, J. Theor. Biol. 254 (2008) 861.
[29] T. Rungrotmongkol, N. Nunthaboot, M. Malaisree, N. Kaiyawet, P. Intharathep, A. Meepraset, S. Hannongbua, J. Mol. Graph. Model. 29 (2010) 347.
[30] Y. Duan et al., J. Comput. Chem. 24 (2003) 1999.
[31] M.B. Tessier, M.L. DeMarco, A.B. Yongye, R.J. Woods, Mol. Simul. 34 (2008) 349.
[32] D.A. Case et al., AMBER 10, San Francisco, 2008.